

Electron-mediated projective quantum nondemolition measurement on a nuclear spin

Wang Ping,^{1,2,3} Wen Yang,^{2,*} and Renbao Liu^{3,†}

¹College of Education for the future, Beijing Normal University, Zhuhai 519087, China

²Beijing Computational Science Research Center, Beijing 100193, China

³Department of Physics, Centre for Quantum Coherence,
and The Hong Kong Institute of Quantum Information Science and Technology,
The Chinese University of Hong Kong, Shatin, New Territories, Hong Kong, China

Projective quantum nondemolition (QND) measurement is important for quantum technologies. Here we propose a method for constructing projective QND measurement on a nuclear spin via the measurement of an axillary electron spin in generic electron-nuclear spin systems coupled through weak hyperfine interaction. The key idea is to apply suitable quantum control on the electron to construct a weak QND measurement on the nuclear spin and then cascade a sequence of such measurements into a projective one. We identify a set of tunable parameters to select the QND observables and control the strength of the weak QND measurement. We also find that the QND measurement can be stabilized against realistic experimental control errors. As a demonstration of our method, we design projective QND measurement on a ¹³C nuclear spin weakly coupled to a nitrogen-vacancy center electron spin in diamond.

INTRODUCTION

Measurement backaction [1] is the measurement-induced non-unitary disturbance on the system being measured. To overcome the downgrade of measurement precision caused by the random disturbance, quantum nondemolition (QND) was introduced [2–7]. The key idea is to measure an observable that is conserved during the free evolution, so that its value remains unaffected between successive measurements and sufficient statistics can be build up to improve the signal-to-noise ratio [8]. QND has been demonstrated experimentally in quantum optics [9], microscopic superconducting systems [10] and trapped single electron [11].

In hybrid electron-nuclear spin systems, the nuclear spin qubits can be exploited as quantum resources due to their long coherence times [12–27]. Projective QND measurement on the nuclear spin qubits is important for scalable quantum computation [28], quantum sensing [20, 21] and quantum communication [29]. The quantum measurement of the nuclear spin is difficult and is often realized indirectly via measurement of a nearby electron spin [30, 31], e.g., mapping the population of a *nearby* nuclear spin onto the electron spin via controlled-NOT gates allows projective QND measurements of the nuclear spin z component \hat{I}_z – a conserved observable protected by the external magnetic field [30, 31]. However, *remote* nuclear spins weakly coupled to the electron (i.e., coupling strength $< 1/T_2^*$) can hardly be resolved or manipulated to implement the controlled-NOT gates reliably. Moreover, the transverse components (I_x, I_y) of the nuclear spin are *not* conserved, so their projective QND measurements are non-trivial. Recently, single-shot readout of nuclear a spin-1/2 weakly coupled to an nitrogen-vacancy center electron spin in diamond was demonstrated experimentally by using a series of weak measurements to trap the target nuclear spin and then read out its state repeatedly [32], but its connection to QND remains unclear.

In this paper, we propose a general method to construct projective QND measurements on *non-conserved* observables

(e.g., the transverse components) of a nuclear spin *weakly* coupled to an axillary electron spin via hyperfine interaction. The procedure consists of two steps. First, dynamical decoupling control is applied to the electron spin to establish electron-nuclear entanglement, followed by a projective measurement on the electron spin to mediate a single weak measurement on the nuclear spin. Second, we apply a sequence of such weak measurements to the nuclear spin and tune the evolution of the nuclear spin between neighboring measurements to meet the stroboscopic QND condition [4, 6, 7, 33–38], so that this sequence of weak QND measurements form a single projective QND measurement on the nuclear spin. We identify a set of tunable parameters for flexible, *in situ* control of the QND observable and find optimal parameters to stabilize the QND measurements against control errors. This work is relevant to state preparation, quantum sensing, and quantum error correction via projective QND measurements.

The paper is organized as follows. In Sec. II, we construct a single weak measurement on the nuclear spin via measurement of the electron spin. In Sec. III, we use a sequence of weak QND measurements to form a single projective QND measurement and analyze its stability against control errors. In Sec. IV, we illustrate our method in a paradigmatic physical system, i.e., a ¹³C nuclear spin weakly coupled to a nitrogen-vacancy center electron spin in diamond [32]. In Sec. V, we draw the conclusions.

ELECTRON-MEDIATED MEASUREMENT ON NUCLEAR SPIN

We consider a target nuclear spin-1/2 $\hat{\mathbf{I}}$ with Zeeman Hamiltonian $\omega_n \hat{I}_z$ coupled to an axillary electron spin with Hamiltonian $\omega_0 \hat{S}_z$ through the hyperfine interaction. The hyperfine interaction is usually much weaker than $|\omega_0|$, so it does not cause electron spin flip and hence can be written as $|+_z\rangle\langle+_z| \mathbf{a}_+ \cdot \hat{\mathbf{I}} + |-_z\rangle\langle-_z| \mathbf{a}_- \cdot \hat{\mathbf{I}}$, where $|\pm_z\rangle$ are the two eigenstates of the electron spin \hat{S}_z . In the interaction picture of the

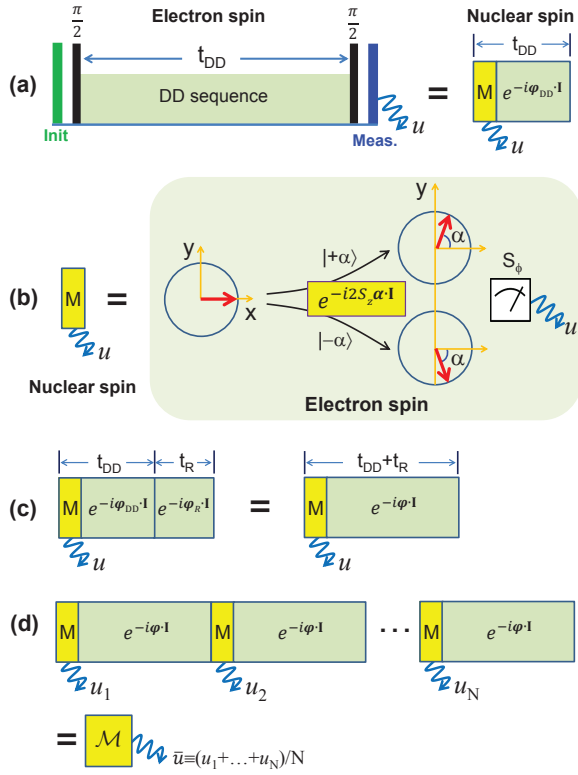


FIG. 1. (a) Control sequence on an auxiliary electron spin coupled to the target nuclear spin via hyperfine interaction. This mediates an effective measurement (yellow box “M”) on the target nuclear spin followed by a rotation $e^{-i\varphi_{DD}\cdot\hat{\mathbf{I}}}$. (b) The effective measurement on the nuclear spin originates from the conditional rotation of the electron spin (red arrows) around the z axis by opposite angles for opposite nuclear spin initial states $|\pm\alpha\rangle$ – the two eigenstates of $\hat{\alpha}\cdot\hat{\mathbf{I}}$, and the subsequent projective measurement on the electron spin observable $\hat{S}_\phi \equiv \hat{\mathbf{S}}\cdot\mathbf{e}_\phi$, where $\mathbf{e}_\phi = \mathbf{e}_x \cos\phi + \mathbf{e}_y \sin\phi$. (c) Immediately after the \hat{S}_ϕ measurement, we re-initialize the electron spin into $|+\rangle$ and append a waiting time t_R , during which we flip the electron spin to engineer the nuclear spin evolution $e^{-i\varphi_R\cdot\hat{\mathbf{I}}}$. The total evolution of the nuclear spin after the measurement becomes $e^{-i\varphi\cdot\hat{\mathbf{I}}} \equiv e^{-i\varphi_R\cdot\hat{\mathbf{I}}}e^{-i\varphi_{DD}\cdot\hat{\mathbf{I}}}$. (d) Cascading N weak measurements with outcome (u_1, \dots, u_N) into a single strong measurement with outcome $\bar{u} \equiv (u_1 + \dots + u_N)/N$.

electron spin, the total Hamiltonian takes the form

$$\hat{H} = \omega \cdot \hat{\mathbf{I}} + \hat{S}_z \mathbf{A} \cdot \hat{\mathbf{I}}, \quad (1)$$

with $\omega \equiv \omega_n \mathbf{e}_z + (\mathbf{a}_+ + \mathbf{a}_-)/2$ the hyperfine-shifted nuclear Larmor frequency and $\mathbf{A} \equiv \mathbf{a}_+ - \mathbf{a}_-$ the effective hyperfine interaction.

Theoretical formalism

The protocol for constructing a single electron-mediated weak measurement on the nuclear spin is shown in Fig. 1(a). At $t = 0$, the electron spin starts from the spin-up state $|+\rangle_z$ along the $+z$ axis, while the nuclear spin starts from a general initial state $\hat{\rho}$. Next, a $\pi/2$ -pulse around the y axis is applied to the electron spin to rotate it to the $\hat{S}_x = +1/2$ eigenstate $|+\rangle_x$. Next a dynamical decoupling (DD) sequence is applied to the electron spin to generate the evolution

$$\hat{U}_{DD} = e^{-i\varphi_{DD}\cdot\hat{\mathbf{I}}} e^{-i2\hat{S}_z\alpha\cdot\hat{\mathbf{I}}}, \quad (2)$$

driving the electron-nuclear system into the entangled state $\hat{U}_{DD}|+\rangle_x \hat{\rho} \langle +|_x \hat{U}_{DD}^\dagger$. Here φ_{DD} and α are vectors that depend on the hyperfine interaction \mathbf{A} and the DD sequence (see Appendix A). Finally a projective measurement is made on the electron spin $\hat{S}_\phi \equiv \hat{\mathbf{S}}\cdot\mathbf{e}_\phi$ along $\mathbf{e}_\phi \equiv \mathbf{e}_x \cos\phi + \mathbf{e}_y \sin\phi$ by first applying a $\pi/2$ -pulse along $\mathbf{e}_{\phi-\pi/2}$ to rotate \hat{S}_ϕ to \hat{S}_z and then measuring \hat{S}_z . Upon getting a specific outcome u ($= +$ or $-$), the *nuclear spin* collapses into the u -dependent (unnormalized) final state

$$\langle u_\phi | \hat{U}_{DD} | + \rangle_x \hat{\rho} \langle + |_x \hat{U}_{DD}^\dagger | u_\phi \rangle = e^{-i\varphi_{DD}\cdot\hat{\mathbf{I}}} \hat{M}_u \hat{\rho} (\hat{M}_u)^\dagger e^{i\varphi_{DD}\cdot\hat{\mathbf{I}}}, \quad (3)$$

where $|\pm_\phi\rangle$ are the two eigenstates of the electron spin \hat{S}_ϕ and

$$\hat{M}_u \equiv \langle u_\phi | e^{-i2\hat{S}_z\alpha\cdot\hat{\mathbf{I}}} | + \rangle_x = \frac{e^{i(\alpha\cdot\hat{\mathbf{I}}-\phi/2)} + u e^{-i(\alpha\cdot\hat{\mathbf{I}}-\phi/2)}}{2} \quad (4)$$

is the u -dependent Kraus operator acting on the *nuclear spin*. When $\phi = 0$, $\{\hat{M}_u\}$ reduce to those in Ref. [39].

The nuclear spin evolution from $\hat{\rho}$ at $t = 0$ to the \hat{u} -dependent final state [Eq. (3)] consists of a measurement followed by a unitary rotation $e^{-i\varphi_{DD}\cdot\hat{\mathbf{I}}}$ [see Fig. 1(a)]. The measurement is described by the positive-operator valued measure (POVM) set $\{\hat{M}_\pm\}$, i.e., outcome u occurs with probability

$$P(u) = \text{Tr} \hat{M}_u \hat{\rho} \hat{M}_u^\dagger = P(u|\alpha) \langle \alpha | \hat{\rho} | \alpha \rangle + P(u|-\alpha) \langle -\alpha | \hat{\rho} | -\alpha \rangle$$

and collapses the nuclear spin into $\hat{M}_u \hat{\rho} \hat{M}_u^\dagger$, where

$$P(u|\pm\alpha) = \frac{1 + u \cos(\phi \mp \alpha)}{2} \quad (5)$$

is the conditional probability of outcome u for the nuclear spin initial state $|\pm\alpha\rangle$. In the above, we have defined $\alpha \equiv |\alpha|$, $\hat{\alpha} \equiv \alpha/\alpha$, and used $|\pm\alpha\rangle$ for the eigenstates of $\hat{\alpha}\cdot\hat{\mathbf{I}}$ with eigenvalue $\pm 1/2$.

Physical picture

The measurement on the target nuclear spin is constructed by first entangling it with an ancillary electron spin via the DD-generated evolution $e^{-i2\hat{S}_z\alpha\cdot\hat{\mathbf{I}}}$ and then measuring this electron spin. As shown in Fig. 1(b), the evolution $e^{-i2\hat{S}_z\alpha\cdot\hat{\mathbf{I}}}$ is a nuclear-controlled rotation of the electron spin around the z

axis: for opposite nuclear spin initial states $|\pm\alpha\rangle$, it rotates the electron spin from $|+_x\rangle$ to $|\pm\alpha\rangle_e \equiv e^{\mp i\alpha\hat{S}_z}|+_x\rangle$. This correlates the two orthogonal eigenstates $|\pm\alpha\rangle$ of the nuclear spin observable $\hat{\alpha} \cdot \hat{\mathbf{I}}$ with *distinct* (but not necessarily orthogonal) final states $|\pm\alpha\rangle_e$ of the electron spin. In the subsequent measurement on the electron spin, $|\pm\alpha\rangle_e$ in turn give *distinct* measurement distributions $P(u|\pm\alpha)$, i.e., measuring the electron spin can distinguish (partially) between $|\pm\alpha\rangle_e$ or equivalently between $|\pm\alpha\rangle$. So measuring the electron spin observable \hat{S}_ϕ mediates a (partial) measurement on the nuclear spin observable $\hat{\alpha} \cdot \hat{\mathbf{I}}$. The strength of the measurement on the nuclear spin is quantified by the degree to which this measurement can distinguish between the two eigenstates $|\pm\alpha\rangle$ of $\hat{\alpha} \cdot \hat{\mathbf{I}}$, i.e., the distinguishability between $P(u|\pm\alpha)$.

Quantitatively, we characterize $P(u|a)$ ($a = \pm\alpha$) by the conditional expectation value of the measurement outcome

$$\langle u \rangle_a \equiv P(+|a) - P(-|a) = \cos(\phi - a) \quad (6)$$

and its fluctuation

$$\sigma_a \equiv \sqrt{\langle u^2 \rangle_a - \langle u \rangle_a^2} = |\sin(\phi - a)|. \quad (7)$$

We identify $\langle u \rangle_a - \langle u \rangle_{-a}$ and $\sigma_a + \sigma_{-a}$, respectively, as the ‘‘signal’’ and ‘‘noise’’ for distinguishing between the two eigenstates $|\pm\alpha\rangle$ of $\hat{\alpha} \cdot \hat{\mathbf{I}}$ and define the distinguishability between $P(u|\pm\alpha)$ or equivalently the strength of the measurement on $\hat{\alpha} \cdot \hat{\mathbf{I}}$ as the signal-to-noise ratio:

$$D \equiv \frac{\langle u \rangle_\alpha - \langle u \rangle_{-\alpha}}{\sigma_\alpha + \sigma_{-\alpha}} = \min\{|\tan \alpha|, |\tan \phi|\}. \quad (8)$$

Here $\tan \alpha$ characterizes the difference between $|\pm\alpha\rangle_e$ or equivalently the degree of electron-nuclear entanglement, while $\tan \phi$ characterizes the degree to which measuring the electron spin observable \hat{S}_ϕ can distinguish between $|\pm\alpha\rangle_e$ and hence $|\pm\alpha\rangle$. For example, $\tan \alpha \approx 0$ leads to $|\pm\alpha\rangle_e \approx |-\alpha\rangle_e$ up to a phase factor, so any measurement on the electron spin always yields $P(u|\pm\alpha) \approx P(u|-\alpha)$ and $D \approx 0$, i.e., weak measurement on the nuclear spin. For a given α , measuring \hat{S}_y (i.e., $\phi = \pi/2$) can optimally distinguish $|\pm\alpha\rangle_e$ by yielding maximally different $P(u|\pm\alpha)$, so it gives maximal measurement strength. By contrast, measuring \hat{S}_x (i.e., $\phi = 0$) cannot distinguish $|\pm\alpha\rangle_e$ since it always gives $P(u|\pm\alpha) = P(u|-\alpha)$, so it leads to vanishing measurement strength: $D = 0$.

In the above, we have assumed ideal projective measurement on the electron spin observable \hat{S}_ϕ . If this measurement is not perfect, as quantified by a finite probability p_\pm to get an outcome $u = \pm$ when the true electron spin state is $|\pm\phi\rangle$, then we should replace $\cos(\phi \mp \alpha)$ in Eq. (5) by $\Delta p + \bar{p} \cos(\phi \mp \alpha)$, where $\Delta p \equiv p_+ - p_-$ and $\bar{p} \equiv p_+ + p_- - 1$. This reduces the ‘‘signal’’ by a factor \bar{p} , but increases the ‘‘noise’’, so it weakens the measurement strength to

$$D = \frac{2\bar{p}|\sin \alpha \sin \phi|}{\sum_{a=\pm\alpha} \sqrt{1 - [\Delta p + \bar{p} \cos(\phi - a)]^2}} \stackrel{\bar{p} \ll 1}{\approx} \bar{p}|\sin \alpha \sin \phi|. \quad (9)$$

To summarize, the measurement on the nuclear spin is controlled by two parameters $\alpha = \alpha\hat{\alpha}$ and ϕ , i.e., $\hat{\alpha}$ controls the nuclear spin observable $\hat{\alpha} \cdot \hat{\mathbf{I}}$ being measured, while $\tan \alpha$ and $\tan \phi$ controls the distinguishability D between $P(u|\pm\alpha)$ or equivalently the measurement strength. For example, $\tan \alpha \tan \phi \approx 0$ gives nearly identical $P(u|\pm\alpha)$ and hence $D \approx 0$, while $\alpha = \phi = \pi/2$ gives *non-overlapping* (i.e., perfectly distinguishable) $P(u|\alpha) = \delta_{u,+}$ and $P(u|-\alpha) = \delta_{u,-}$ and hence a projective measurement ($D = \infty$), as described by the POVM set [Eq. (4)] $\hat{M}_+ \equiv |+\alpha\rangle\langle +\alpha|$ and $\hat{M}_- \equiv |-\alpha\rangle\langle -\alpha|$. The parameter ϕ can be tuned directly in the experiment, while the direction and magnitude of α can be tuned *independently* by varying the duration and structure of the DD sequence. Next we discuss this tunability in more detail.

Tunability of α

The tunability of α becomes physically transparent when the perpendicular part \mathbf{A}_\perp of the hyperfine interaction vector \mathbf{A} with respect to ω is much smaller than $|\omega|$. In this case, we obtain approximate analytical expressions (see Appendix B)

$$\varphi_{\text{DD}} \approx \omega t_{\text{DD}}, \quad (10)$$

$$\alpha \approx |f_{\text{DD}}| \mathbb{R}(-\arg(f_{\text{DD}})) \frac{\omega}{|\omega|} \frac{\mathbf{A}_\perp t_{\text{DD}}}{2}, \quad (11)$$

where $\mathbb{R}(\theta)$ is the SO(3) rotation matrix that rotates a vector around the axis θ by an angle $|\theta|$ and

$$f_{\text{DD}} \equiv \frac{1}{t_{\text{DD}}} \int_0^{t_{\text{DD}}} s(t) e^{i\omega t} dt \quad (12)$$

accounts for the DD sequence [40, 41]: $s(t)$ starts from $s(0) = +1$ and switches its sign at the timings of each π -pulse in the DD sequence. The tunability of α is completely characterized by f_{DD} : its phase $\arg(f_{\text{DD}})$ controls the direction of α and hence the nuclear spin observable $\hat{\alpha} \cdot \hat{\mathbf{I}}$ to be measured, while its magnitude $|f_{\text{DD}}|$ controls the magnitude of α and hence the measurement strength. By varying the duration of the DD sequence and the timings of the constituent π -pulses, we can tune $\arg(f_{\text{DD}})$ and $|f_{\text{DD}}|$ independently, e.g., the N_{DD} -period Carr–Purcell–Meiboom–Gill (CPMG) sequence $(\tau/4 - \pi - \tau/2 - \pi - \tau/4)^{N_{\text{DD}}}$ corresponds to $t_{\text{DD}} \equiv N_{\text{DD}}\tau$ and

$$f_{\text{DD}} = -e^{i|\omega|t_{\text{DD}}/2} \frac{4}{|\omega|t_{\text{DD}}} \frac{\sin^2(|\omega|\tau/8) \sin(|\omega|t_{\text{DD}}/2)}{\cos(|\omega|\tau/4)},$$

so $\arg(f_{\text{DD}})$ can be tuned by varying N_{DD} , while $|f_{\text{DD}}|$ can be tuned by varying τ . Setting $\tau = 2\pi/|\omega|$ gives maximal $f_{\text{DD}} = 2/\pi$ and hence maximal $\alpha = \mathbf{A}_\perp t_{\text{DD}}/\pi$.

Equation (11) suggests that the magnitude of α can be enhanced indefinitely by increasing the total duration t_{DD} of the DD sequence. In practice, however, the ancillary electron spin, albeit under the DD control, still has a finite coherence time T_2 , which sets an upper limit $t_{\text{DD}} \lesssim T_2$ and hence $\alpha \lesssim |\mathbf{A}_\perp|T_2/2$ since $|f_{\text{DD}}| \leq 1$. Here, in addition to providing the desired tunability for α , the DD sequence also filters

out undesirable noises to enhance the electron spin coherence time T_2 beyond the inhomogeneous dephasing time T_2^* . This not only provides a better spectral resolution $1/T_2 \ll 1/T_2^*$ to single out the target nuclear spin among other environmental nuclei [32], but also enhances the maximal achievable measurement strength. As a result, projective measurement (i.e., $\alpha = \phi = \pi/2$) can be achieved even for weakly coupled target nuclear spins with hyperfine interaction $|\mathbf{A}| < 1/T_2^*$, as long as $|\mathbf{A}_\perp| \gtrsim 1/T_2$. For extremely weak hyperfine interaction $|\mathbf{A}_\perp| \lesssim 1/T_2$, the maximal achievable α is less than $\pi/2$, i.e., a single projective measurement on the electron spin can at most mediate a weak measurement on the nuclear spin. Interestingly, even in this case, projective measurement is still possible.

CONSTRUCTION OF PROJECTIVE QND MEASUREMENTS

When only weak measurements are available, a natural idea to construct a projective measurement is to cascade a sequence of weak measurements into a single projective measurement [8, 42]: although each measurement is weak, the two eigenstates $|\pm\alpha\rangle$ of the observable $\hat{\alpha} \cdot \hat{\mathbf{I}}$ being measured can always be distinguished reliably by the statistics of a large number of repeated weak measurements on $|\pm\alpha\rangle$. In our case, however, the weak measurement over $\hat{\alpha} \cdot \hat{\mathbf{I}}$ is always followed by a unitary rotation $e^{-i\varphi_{\text{DD}}\hat{\mathbf{I}}}$. Since φ_{DD} and $\hat{\alpha}$ are usually noncollinear, a naive repetition of the protocol in Fig. 1(a) would not form a projective measurement, because $e^{-i\varphi_{\text{DD}}\hat{\mathbf{I}}}$ may destroy the eigenstates $|\pm\alpha\rangle$ of the observable $\hat{\alpha} \cdot \hat{\mathbf{I}}$ and hence make repeated measurements on $|\pm\alpha\rangle$ impossible. To construct a projective measurement from a sequence of weak measurements, the first step is to protect the eigenstates of $\hat{\alpha} \cdot \hat{\mathbf{I}}$ against the rotation $e^{-i\varphi_{\text{DD}}\hat{\mathbf{I}}}$, i.e., to make each weak measurement QND.

Stroboscopic QND condition

The idea of stroboscopic QND [4, 6, 7, 33–38] is to use *stroboscopic* measurements with precise timings to protect the eigenstates of the observable being measured. For example, under an external magnetic field B along the z axis, the Zeeman Hamiltonian $\hat{H}_0 = \gamma B \hat{S}_z$ of a spin-1/2 drives periodic Larmor precession, so the evolution operator $e^{-i\gamma B \tau \hat{S}_z}$ becomes a c -number when the evolution time τ equals the Larmor precession period $2\pi/(\gamma B)$. If we perform a sequence of stroboscopic measurements with the measurement interval being an integer multiple of the Larmor precession period [34, 36–38], then the evolution between neighboring measurements does not affect the post-measurement state, so the QND condition is satisfied.

Interestingly, although our protocol in Fig. 1(a) is not stroboscopic, it effectively generates a “stroboscopic” measurement on the nuclear spin observable $\hat{\alpha} \cdot \hat{\mathbf{I}}$, but is followed by a

unitary rotation $e^{-i\varphi_{\text{DD}}\hat{\mathbf{I}}}$ that may destroy the eigenstates $|\pm\alpha\rangle$ of $\hat{\alpha} \cdot \hat{\mathbf{I}}$. To protect $|\pm\alpha\rangle$, we re-initialize the electron spin into $|+\rangle_z$ immediately after the \hat{S}_ϕ measurement and then append a waiting time t_R [see Fig. 1(c)]. Since the nuclear spin precession frequency is $\omega \pm \mathbf{A}/2$ when the electron stays in $|\pm\rangle_z$, we can engineer the nuclear spin evolution $e^{-i\varphi_R\hat{\mathbf{I}}}$ during this waiting time by flipping the electron spin between $|\pm\rangle_z$ with π -pulses, e.g., $e^{-i\varphi_R\hat{\mathbf{I}}} = e^{-i(\omega+\mathbf{A}/2)t_R\hat{\mathbf{I}}}$ if we do not flip the electron spin and $e^{-i\varphi_R\hat{\mathbf{I}}} = e^{-i(\omega-\mathbf{A}/2)(t_R-t_1)\hat{\mathbf{I}}}e^{-i(\omega+\mathbf{A}/2)t_1\hat{\mathbf{I}}}$ if we flip the electron spin at t_1 . Since the two rotation axes $\omega \pm \mathbf{A}/2$ are usually non-collinear, we can achieve an *arbitrary* evolution $e^{-i\varphi_R\hat{\mathbf{I}}}$ by tuning t_R and the timings of the electron spin flip. The total evolution of the nuclear spin after each weak measurement becomes

$$e^{-i\varphi\hat{\mathbf{I}}} \equiv e^{-i\varphi_R\hat{\mathbf{I}}}e^{-i\varphi_{\text{DD}}\hat{\mathbf{I}}}. \quad (13)$$

Protecting the eigenstates $|\pm\alpha\rangle$ of $\hat{\alpha} \cdot \hat{\mathbf{I}}$ requires $e^{-i\varphi\hat{\mathbf{I}}}$ to commute with $\hat{\alpha} \cdot \hat{\mathbf{I}}$, or equivalently

$$\text{mod}(|\varphi|, 2\pi) = 0 \quad \text{or} \quad \varphi \parallel \hat{\alpha}. \quad (14)$$

For weak hyperfine interaction and hence $\varphi \perp \hat{\alpha}$, Eq. (14) reduces to $\text{mod}(|\varphi|, 2\pi) = 0$, reminiscent of stroboscopic QND measurements at integer multiples of the system’s period [34, 36–38]. In Eq. (13), $e^{-i\varphi_{\text{DD}}\hat{\mathbf{I}}}$ is determined by the DD sequence [Fig. 1(a)], so the QND condition Eq. (14) imposes different requirements on $e^{-i\varphi_R\hat{\mathbf{I}}}$ for different DD sequences. Due to the complete tunability in $e^{-i\varphi_R\hat{\mathbf{I}}}$, the QND condition is always achievable. Moreover, as we prove in Appendix , for a large class of DD sequences, i.e., when the DD sequence is the repetition of an even-order concatenated DD [43–46] (with the widely-used CPMG sequence $(\tau/4-\pi-\tau/2-\pi-\tau/4)^{N_{\text{DD}}}$ being an example), the QND condition can be achieved by tuning t_R only, without flipping the electron spin during the waiting time.

Under the QND condition, we can repeat the structure in Fig. 1(c) to form a single projective measurement, as shown in Fig. 1(d). In the following, we first describe the gradual formation of a single projective QND measurement from a sequence of weak QND measurements [38, 42] and then discuss its stability against control errors.

Cascading weak measurements into projective measurement

To begin with, we use the eigenstates $|\pm\alpha\rangle$ of the observable $\hat{\alpha} \cdot \hat{\mathbf{I}}$ to rewrite the POVM elements $\{\hat{M}_u\}$ [Eq. (4)] as

$$\hat{M}_u \equiv \sum_{a=\pm\alpha} \sqrt{P(u|a)} e^{i\theta_{u,a}} |a\rangle\langle a|,$$

where $e^{i\theta_{u,a}}$ is a trivial phase factor and $P(u|a)$ is the conditional probability of outcome u for the initial state $|a\rangle$ ($a = \pm\alpha$), see Eq. (5). As discussed at the end of Sec. , weak measurement ($D \ll 1$) corresponds to small difference between $P(u|\pm\alpha)$, so that a single measurement can barely distinguish

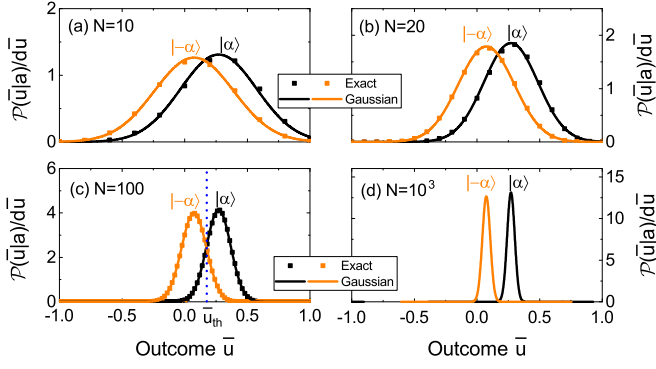


FIG. 2. Conditional distributions $\mathcal{P}(\bar{u} | \pm \alpha)$ for the average $\bar{u} = (1/N) \sum_{i=1}^N u_i$ of N sequential binary measurements with $\alpha = 0.1$ and $\phi = 4\pi/9$, i.e., the strength of each binary measurement is $D \approx 0.1$. Squares for Eq. (15) and solid lines for Eq. (16). The vertical dashed line in (c) marks the optimal threshold \bar{u}_{th} that maximizes the average readout fidelity.

between $|\pm \alpha\rangle$; while a projective measurement ($D \rightarrow \infty$) corresponds to non-overlapping $P(u | \pm \alpha)$, so that a single measurement can perfectly distinguish between $|\pm \alpha\rangle$.

As shown in Fig. 1(d), we consider a sequence of N identical measurements with an outcome $\mathbf{u} \equiv (u_1, \dots, u_N)$, where u_i is the outcome of the i th measurement. To keep our theory general, we do not make any assumptions about the strength of each measurement. The POVM element for these N measurements is $\hat{M}_{\mathbf{u}} \equiv e^{-i\varphi \hat{\mathbf{I}}} \hat{M}_{u_N} \dots e^{-i\varphi \hat{\mathbf{I}}} \hat{M}_{u_1}$, e.g., for an arbitrary initial state $\hat{\rho}$, the probability for outcome \mathbf{u} is $\text{Tr} \hat{M}_{\mathbf{u}} \hat{\rho} \hat{M}_{\mathbf{u}}^\dagger$. Under the QND condition Eq. (14), \hat{M}_+ , \hat{M}_- , and $e^{-i\varphi \hat{\mathbf{I}}}$ mutually commute, so $\hat{M}_{\mathbf{u}} = e^{-iN\varphi \hat{\mathbf{I}}} \hat{M}_+^{N_+} \hat{M}_-^{N_-}$ only depends on the number N_\pm of outcome \pm contained in \mathbf{u} , or equivalently the averaged outcome

$$\bar{u} \equiv \frac{N_+ - N_-}{N} = \frac{1}{N} \sum_{i=1}^N u_i,$$

which takes discrete values in $[-1, +1]$ evenly spaced by $d\bar{u} \equiv 2/N$. This allows us to regard the N sequential measurements with outcome \mathbf{u} as a *single* effective measurement with outcome \bar{u} [Fig. 1(d)], without losing any information about the post-measurement state. Since each constituent measurement gives a binary-valued outcome $u = +$ or $-$, while the resulting effective measurement gives a multi-valued outcome \bar{u} , we call the former *binary* measurement and the latter *multi-outcome* measurement to avoid confusion. Since there are $N!/(N_+!N_-!)$ distinct \mathbf{u} 's that give the same \bar{u} , the POVM element for the multi-outcome measurement is

$$\hat{M}_{\bar{u}} \equiv \sqrt{\frac{N!}{N_+!N_-!}} \hat{M}_{\mathbf{u}} = \sum_{a=\pm\alpha} \sqrt{\mathcal{P}(\bar{u}|a)} e^{i\Theta_{\bar{u},a}} |a\rangle\langle a|,$$

where $e^{i\Theta_{\bar{u},a}}$ is a trivial phase factor and

$$\mathcal{P}(\bar{u}|a) \equiv N! \frac{[P(+|a)]^{N_+}}{N_+!} \frac{[P(-|a)]^{N_-}}{N_-!} \quad (15)$$

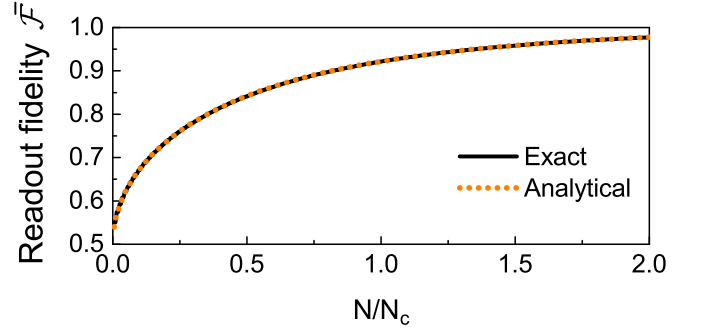


FIG. 3. Average readout fidelity $\bar{\mathcal{F}}$ of the multi-outcome measurement as a function of the number N (in units of $N_c \equiv 2/D^2$) of constituent binary measurements. Here $\phi = \pi/2$ and $\alpha = 0.1$, i.e., the strength of each binary measurement is $D = 0.1$.

is the probability of outcome \bar{u} conditioned on the initial state being $|a\rangle$ ($a = \pm\alpha$). When $N \gg 1$, the conditional distribution of \bar{u} becomes Gaussian (see Fig. 2):

$$\mathcal{P}(\bar{u}|a) \approx \frac{e^{-(\bar{u}-\langle u \rangle_a)^2 / (2\sigma_a^2/N)}}{\sqrt{2\pi}\sigma_a / \sqrt{N}} d\bar{u}. \quad (16)$$

According to Eq. (16), the averaged outcome \bar{u} of N binary measurements has the same conditional expectation value as that of each binary measurement [Eq. (6)], while its conditional fluctuation is \sqrt{N} times smaller [cf. Eq. (7)], consistent with the central limit theorem. As a result, the distinguishability (denoted by \mathcal{D}) between $\mathcal{P}(\bar{u} | \pm \alpha)$ or equivalently the strength of the multi-outcome measurement is \sqrt{N} times that of each binary measurement:

$$\mathcal{D}(N) \equiv \sqrt{N}D. \quad (17)$$

Physically, under the QND condition, the eigenstates $|\pm \alpha\rangle$ of the observable $\hat{\alpha} \cdot \hat{\mathbf{I}}$ are simultaneous eigenstates of $\{\hat{M}_u\}$ and $e^{-i\varphi \hat{\mathbf{I}}}$, so it remains invariant during the sequential measurements. This allows $|\pm \alpha\rangle$ to be measured repeatedly to improve the distinguishability between $\mathcal{P}(\bar{u} | \pm \alpha)$: the signal-to-noise ratio provided by $\bar{u} - \langle \bar{u} \rangle$ – the average of N binary outcomes – is \sqrt{N} times that of a single binary outcome u .

For sufficiently large N and hence D , the two curves $\mathcal{P}(\bar{u} | \pm \alpha)$ have negligible overlap, see Fig. 2(d) for an example. Then an outcome \bar{u}_0 lies under either $\mathcal{P}(\bar{u}|a)$ or $\mathcal{P}(\bar{u}|-a)$, so a *single* outcome \bar{u}_0 is sufficient for a reliable discrimination of $|\pm \alpha\rangle$, i.e., \bar{u}_0 under $\mathcal{P}(\bar{u}|a)$ ($a = \pm\alpha$) indicates the initial state to be $|a\rangle$. Correspondingly, the multi-outcome measurement becomes projective: $\hat{M}_{\bar{u}_0} \propto |a\rangle\langle a|$ for \bar{u}_0 under $\mathcal{P}(\bar{u}|a)$.

For finite N , the conditional distributions $\mathcal{P}(\bar{u} | \pm \alpha)$ always have a finite overlap. In this case, we can introduce a threshold \bar{u}_{th} lying between $\langle u \rangle_\alpha$ and $\langle u \rangle_{-\alpha}$ [see Fig. 2(c) for an example] and identify the initial state as $|a\rangle$ ($a = \pm\alpha$) if \bar{u} lies on the side of $\langle u \rangle_a$. This identification is correct if the outcome \bar{u} lies outside the overlapping region, but it could be incorrect if \bar{u} lies inside the small overlapping region. To quantify its accuracy, we define the readout *fidelity* \mathcal{F}_a of the state $|a\rangle$

($a = \pm\alpha$) as the probability to identify the initial state to be $|\alpha\rangle$ when the true initial state is $|\alpha\rangle$, e.g., $\mathcal{F}_\alpha = \sum_{\bar{u} > \bar{u}_{\text{th}}} \mathcal{P}(\bar{u}|\alpha)$ and $\mathcal{F}_{-\alpha} \equiv \sum_{\bar{u} < \bar{u}_{\text{th}}} \mathcal{P}(\bar{u}|\alpha)$ for $\langle u \rangle_\alpha > \langle u \rangle_{-\alpha}$. Ideal projective measurement corresponds to $\mathcal{F}_{\pm\alpha} = 1$. Following Refs. [30, 47], we maximize the average readout fidelity $\bar{\mathcal{F}} \equiv (\mathcal{F}_\alpha + \mathcal{F}_{-\alpha})/2$ by setting \bar{u}_{th} at the overlapping point, see the vertical dotted lines in Fig. 2(c). For $N \gg 1$, $\mathcal{P}(\bar{u}|\pm\alpha)$ are approximately Gaussian [Eq. (16)], then

$$\bar{u}_{\text{th}} \approx \frac{\langle u \rangle_\alpha / \sigma_\alpha + \langle u \rangle_{-\alpha} / \sigma_{-\alpha}}{1/\sigma_\alpha + 1/\sigma_{-\alpha}},$$

so the readout fidelity

$$\bar{\mathcal{F}} = \mathcal{F}_{\pm\alpha} \approx \frac{1}{2} + \frac{1}{2} \operatorname{erf}\left(\frac{\mathcal{D}}{\sqrt{2}}\right) \quad (18)$$

is a *universal* function of the distinguishability \mathcal{D} [Eq. (17)] between $\mathcal{P}(\bar{u}|\pm\alpha)$ or equivalently measurement strength. As shown in Fig. 3, Eq. (18) agrees well with the exact results. When $\mathcal{D} \gtrsim 1$, $\bar{\mathcal{F}}$ approaches 100%, so the multi-outcome measurement approaches an ideal projective measurement. For example, $N = N_c \equiv 2/D^2$ leads to $\mathcal{D} = \sqrt{2}$ and hence $\bar{\mathcal{F}} \approx 92\%$, while $N = 2N_c$ leads to $\mathcal{D} = 2$ and hence $\bar{\mathcal{F}} \approx 98\%$.

For clarity, in the following we define $\bar{\mathcal{F}}_{\text{th}} \equiv 92\%$ or equivalently $\mathcal{D}_{\text{th}} \equiv \sqrt{2}$ as the *threshold* of a high-fidelity projective measurement.

Stability analysis

When the QND condition Eq. (14) is violated slightly, the rotation $e^{-i\varphi\hat{\mathbf{I}}}$ after each binary measurement will rotate the eigenstates $|\pm\alpha\rangle$ of the observable $\hat{\alpha} \cdot \hat{\mathbf{I}}$ slightly away from the measurement axis $\hat{\alpha}$, then the initial state $|\pm\alpha\rangle$ is destroyed after certain number (denoted by N_L – the “lifetime” of $|\pm\alpha\rangle$) of binary measurements. Then the initial state $|\pm\alpha\rangle$ can be measured repeated by at most N_L binary measurements, so the strength of the resulting multi-outcome measurement can reach at most $\mathcal{D}(N_L) = \sqrt{N_L} \mathcal{D}$. Then constructing a projective measurement above the threshold fidelity $\bar{\mathcal{F}}_{\text{th}} \equiv 92\%$ requires $\mathcal{D}(N_L) \geq \mathcal{D}_{\text{th}} \equiv \sqrt{2}$ or equivalently long lifetime

$$N_L \gtrsim N_c \equiv \frac{2}{D^2}. \quad (19)$$

For a quantitative discussion, we calculate the *unconditional* (i.e., with the measurement outcomes discarded) survival probability of $|\pm\alpha\rangle$ after a sequence of N binary measurements, with the i th measurement followed by the rotation $e^{-i\delta\varphi_i\hat{\mathbf{I}}}$. A binary measurement with outcome discarded changes a general nuclear spin state $\hat{\rho} = 1/2 + \hat{\mathbf{I}} \cdot \mathbf{n}$ with polarization \mathbf{n} into $\sum_u \hat{M}_u \hat{\rho} \hat{M}_u^\dagger = 1/2 + \hat{\mathbf{I}} \cdot \mathbb{M} \mathbf{n}$, where $\mathbb{M} \equiv [\mathbb{R}(\alpha) + \mathbb{R}(-\alpha)]/2$ describes the measurement-induced dephasing and $\mathbb{R}(\theta)$ is the SO(3) rotation matrix as defined after Eq. (11). The effect of \mathbb{M} is to reduce the polarization components perpendicular to $\hat{\alpha}$ by a factor $\cos\alpha$. For clarity we take the

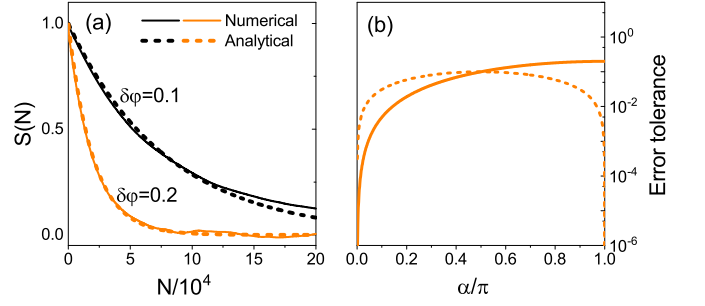


FIG. 4. (a) Stability $S(N)$ of $|\alpha\rangle$ against small systematic rotation error for $\alpha = (\pi - 0.1)\mathbf{e}_{\pi/4}$ and $\phi = -\pi/2$. (b) Tolerance against systematic error (solid line) and uncorrelated random error (dashed line) for electron spin readout fidelity $p = 0.1$.

initial state as $|\alpha\rangle$. At the end of the evolution, the unconditional nuclear spin state $\hat{\rho}(N) = 1/2 + \hat{\mathbf{I}} \cdot \hat{\alpha}(N)$ is characterized by the polarization

$$\hat{\alpha}(N) = \mathbb{R}(\delta\varphi_N)\mathbb{M} \cdots \mathbb{R}(\delta\varphi_1)\mathbb{M}\hat{\alpha}$$

and the survival probability of $|\alpha\rangle$ is

$$\langle \alpha | \hat{\rho}(N) | \alpha \rangle = \frac{1 + \hat{\alpha} \cdot \hat{\alpha}(N)}{2} \equiv \frac{1 + S(N)}{2}.$$

For $|\alpha\rangle$ as the initial state, we obtain the same survival probability. We define the lifetime N_L of $|\pm\alpha\rangle$ as the characteristic N for $S(N)$ to decay to $1/e$. In general, numerical calculations are necessary to determine $S(N)$ and hence N_L .

The QND-breaking effect, i.e., the limitation to the lifetime N_L , originates from the perpendicular component of $\{\delta\varphi_i\}$ with respect to the measurement axis $\hat{\alpha}$. The *worst case* arises if $\{\delta\varphi_i\}$ are all along the same direction (so that different rotations $e^{-i\delta\varphi_i\hat{\mathbf{I}}}$ add up constructively) and this direction is perpendicular to $\hat{\alpha}$ (so that each rotation rotates $|\pm\alpha\rangle$ away from the measurement axis $\hat{\alpha}$ most efficiently). Interestingly, in this worst case, we can obtain analytical results. For clarity we define $\hat{\alpha}$ as the $+X$ axis and $\delta\varphi_i$ as the $+Z$ axis, then $\delta\varphi_i = \delta\varphi_i \mathbf{e}_Z$. We begin with two special cases:

$$S(N) = \begin{cases} \cos\left(\sum_{i=1}^N (-1)^i \delta\varphi_i\right) & \cos\alpha = -1, \\ \prod_{i=1}^N \cos(\delta\varphi_i) & \cos\alpha = 0. \end{cases}$$

The case $\cos\alpha = -1$ corresponds to $\mathbb{M} = \mathbb{R}(\pi\mathbf{e}_X)$, i.e., each binary measurement causes π -rotation of the nuclear spin around the X axis. Then, two binary measurements can reverse a rotation $\mathbb{R}(\delta\varphi\mathbf{e}_Z)$ around the Z axis: $\mathbb{M}\mathbb{R}(\delta\varphi\mathbf{e}_Z)\mathbb{M} = \mathbb{R}(-\delta\varphi\mathbf{e}_Z)$. This measurement-induced spin echo can suppress the decay of $S(N)$ when $\delta\varphi_i$ varies with i slowly. For $\cos\alpha = 0$, the dephasing \mathbb{M} eliminates all the YZ components of the nuclear spin polarization, so the i th binary measurement reduces the length of the polarization by a factor $\cos(\delta\varphi_i)$.

For small systematic rotation error $\delta\varphi_i = \delta\varphi \ll \tan^2(\alpha/2)$, we obtain $S(N) \approx e^{-N(\delta\varphi)^2/[2\tan^2(\alpha/2)]}$, which agrees well with

Parameter sets	P1	P2	P3
Number of CPMG period: N_{DD}	6	6	8
Magnetic field B	691 G	305 G	305 G
Larmor period $T_R \equiv 2\pi/ \omega_n $	1351 ns	3061 ns	3061 ns
Larmor period $T \equiv 2\pi/ \omega $	1088 ns	1936 ns	1936 ns

TABLE I. Three sets of (N_p, B) parameters labelled by P1, P2, and P3. T (T_R) is the period of the Larmor precession during the DD sequence (waiting time) in the weak hyperfine interaction approximation.

the numerical simulations [see Fig. 4(a)]. The lifetime

$$N_L \approx \frac{2}{(\delta\varphi)^2} \tan^2 \frac{\alpha}{2} \quad (20)$$

depends strongly on α and hence the measurement strength of each binary measurement. When the rotation errors $\{\delta\varphi_i\}$ are small uncorrelated random numbers with standard deviation $\delta\varphi$, we obtain $S(N) = e^{-N(\delta\varphi)^2/2}$, so the lifetime

$$N_L = \frac{2}{(\delta\varphi)^2} \quad (21)$$

is independent of α . The condition Eq. (19) for constructing a projective measurement above the threshold fidelity $\bar{\mathcal{F}}_{th} \equiv 92\%$ becomes $\delta\varphi \leq \Delta\varphi$, where

$$\Delta\varphi \equiv \begin{cases} D |\tan(\alpha/2)| & \text{(systematic error)} \\ D & \text{(uncorrelated random error)} \end{cases}, \quad (22)$$

is the tolerance to rotation errors. As shown in Fig. 4(b), for small α , the binary measurement strength $D \propto \alpha$, so the tolerance against systematic (uncorrelated random) rotation error increases quadratically (linearly) with α . For $\alpha \rightarrow \pi$, the measurement strength $D \rightarrow 0$ linearly, so the tolerance against uncorrelated random rotation error also approaches zero linearly. By contrast, when $\alpha \rightarrow \pi$, the lifetime N_L due to systematic rotation error diverges quadratically [see Eq. (20)] due to the measurement-induced spin echo, so the tolerance against systematic rotation error approaches a constant $\Delta\varphi \approx 2\bar{p}$ (for $\bar{p} \ll 1$).

When the DD sequence is the repetition of an even-order concatenated DD, the QND condition can be satisfied by tuning t_R only, without flipping the electron spin during the waiting time [see the discussions after Eq. (14)]. In this case, we have $\varphi_R = (\omega + \mathbf{A}/2)t_R$. Then the rotation error $\delta\varphi \sim \delta\varphi_R = |\omega + \mathbf{A}/2|\delta t_R$ traces back to the error δt_R in controlling the waiting time. The tolerance against rotation error also translates to the tolerance against the waiting time:

$$\Delta t_R \sim \frac{\Delta\varphi}{|\omega + \mathbf{A}/2|}. \quad (23)$$

EXAMPLE: NITROGEN-VACANCY CENTER

We take an nitrogen-vacancy (NV) center electron spin-1 \hat{S}_{NV} coupled to a ^{13}C nuclear spin-1/2 \hat{I} via the hyperfine interaction

$\hat{S}_{NV}^z \mathbf{A} \cdot \hat{I}$ as a paradigmatic physical system to illustrate our method. Under an external magnetic field B along the N-V symmetry axis (defined as the z axis), we can single out two NV electron spin states $|+\rangle \equiv |m_S = 0\rangle$ and $|-\rangle \equiv |m_S = -1\rangle$ to form the auxiliary electron spin-1/2, e.g., $\hat{S}_z \equiv |+\rangle\langle+| - |-\rangle\langle-|$. Then, in the interaction picture of the electron spin-1/2, we recover the total Hamiltonian in Eq. (1). The hyperfine-shifted nuclear Larmor frequency is $\omega \equiv \omega_n \mathbf{e}_z - \mathbf{A}/2$, where $\omega_n \equiv \gamma_n B$ and $\gamma_n = -10.71 \text{ MHz/T}$ is the gyromagnetic ratio of the ^{13}C nucleus. Next, we follow the standard steps to construct a projective QND measurement on the target ^{13}C nucleus.

Electron-mediated measurement on ^{13}C nucleus

We use the protocol in Fig. 1(a) to construct a single binary measurement on the ^{13}C nucleus. We take the DD sequence as the N_{DD} -period CPMG sequence $(\tau/4 - \pi - \tau/2 - \pi - \tau/4)^{N_{DD}}$ and set $\phi = \pi/2$ (i.e., we measure the electron spin observable \hat{S}_y) to maximize the strength of each binary measurement. The fidelity of the fluorescence-based readout of the NV center electron spin is determined by the average photon number n_{\pm} for the electron spin state $|\pm\rangle$ or equivalently the average photon number $\bar{n} = (n_+ + n_-)/2$ and the fluorescence contrast $C \equiv (n_+ - n_-)/(n_+ + n_-)$. Room-temperature experiments have $n_- < n_+ \ll 1$, so nonzero (zero) photon detection corresponds to the outcome $u = +$ ($u = -$). The readout fidelities for $|\pm\rangle$ are $p_+ = n_+$ and $p_- = 1 - n_-$, then $\Delta p = 2\bar{n} - 1$ and $\bar{p} = 2\bar{n}C \ll 1$. Then strength of each binary measurement follows from Eq. (9) as

$$D \approx \sqrt{\bar{n}}C |\sin \alpha| \approx 0.05 |\sin \alpha|, \quad (24)$$

where we have used typical values $n_+ = 0.1$ and $n_- = 0.7n_+$ or equivalently $\bar{n} = 0.085$ and $C = 0.18$ in the last step. At low temperature, using resonant optical excitation [29, 47–51] gives $n_+ \gg n_-$ and hence much higher readout fidelities on the NV electron spin, then Eq. (9) gives

$$D \sim \bar{p} |\sin \alpha| \approx 0.9 |\sin \alpha|, \quad (25)$$

where we have used typical values $p_+ \approx 0.89$ and $p_- \approx 0.99$ in the last step. Thus the measurement strength at low temperature is stronger than that at room temperature by a factor ~ 18 . For specificity, here we consider experiments at *room temperature*.

QND condition and controlling parameters

We use the protocol in Fig. 1(c) to make each binary measurement QND. According to the discussions after Eq. (14), after measuring the electron spin, we immediately re-initialize the electron spin into $|+\rangle = |m_S = 0\rangle$ and then let the ^{13}C nuclear spin undergo free precession $e^{-i\varphi_R \hat{I}} = e^{-i\omega_n t_R \hat{I}_z}$ during the waiting time t_R . The total rotation of the nuclear spin after the

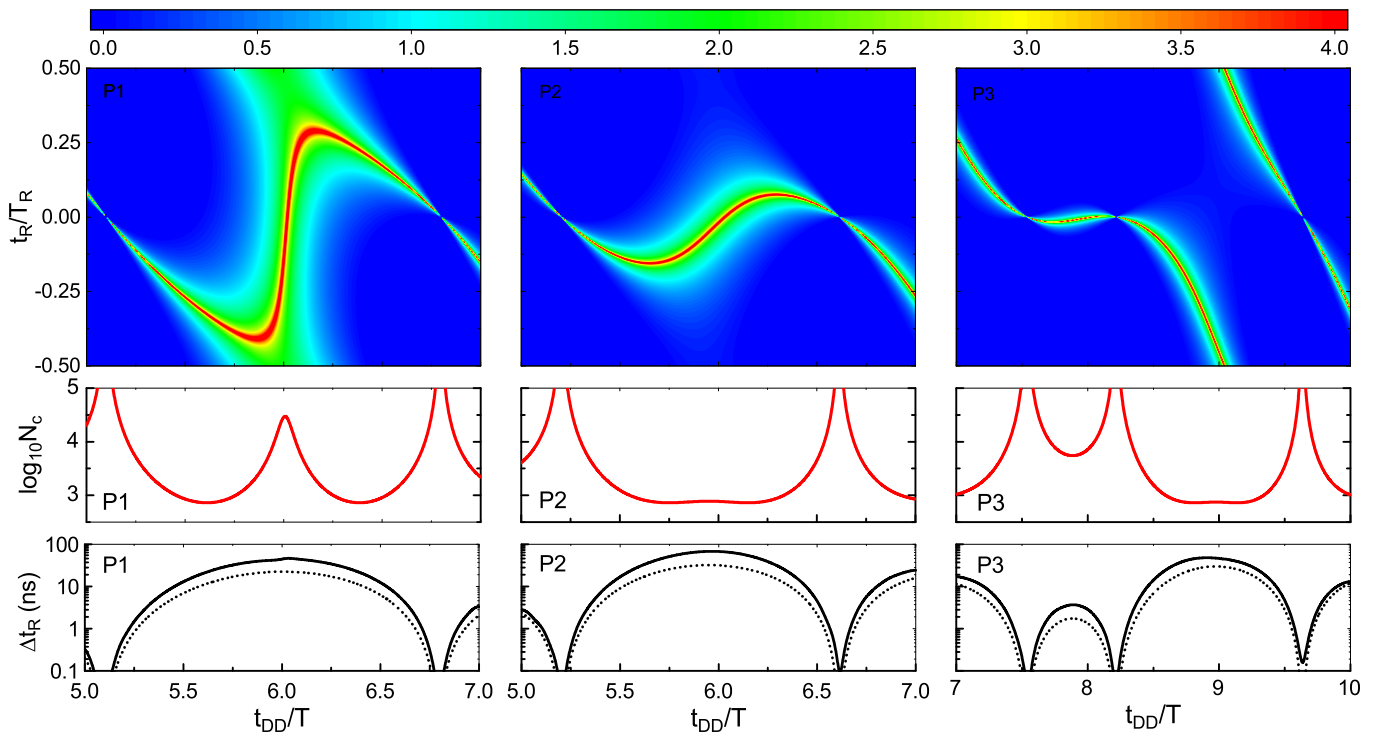


FIG. 5. Upper panels: contour of $\log_{10} N_L$ for P1-P3 in the $(t_{DD}/T, t_R/T_R)$ plane. Middle and lower panels: $\log_{10} N_c$ and error tolerance Δt_R as function of t_{DD}/T . The worst-case estimation for Δt_R is shown as the dashed lines.

binary measurement is $e^{-i\varphi \hat{\mathbf{I}}} \equiv e^{-i\omega_n t_R \hat{I}_z} e^{-i\varphi_{DD} \hat{\mathbf{I}}}$. By varying t_R , we can tune φ towards the QND condition Eq. (14) to provide a sufficiently long lifetime $N_L \geq N_c$ [Eq. (19)], so that we can use N_L repeated binary measurements to form a multi-outcome projective measurement with readout fidelity above the threshold $\mathcal{F}_{th} \equiv 92\%$.

The binary measurement is controlled by α , which depends on the hyperfine interaction \mathbf{A} , the magnetic field B , the number N_{DD} of CPMG periods, and the duration τ of each period. For specificity, we set $\mathbf{A} = (0.316/\sqrt{2}, 0.316/\sqrt{2}, 0.330)$ MHz [32] with $1 \text{ MHz} \equiv 2\pi \times 10^6 \text{ rad}/(\text{s T})$ and consider three sets of (N_{DD}, B) , as labelled by P1, P2, and P3 in Table I. For each set, we still have two controlling parameters: the CPMG sequence period τ (or equivalently the CPMG sequence duration $t_{DD} \equiv N_{DD}\tau$) and the waiting time t_R . With $T \equiv 2\pi/|\omega|$ and $T_R \equiv 2\pi/|\omega_n|$ as the Larmor period of the target ^{13}C nucleus during the CPMG sequence and the waiting time, respectively, we can first tune τ close to resonance with T (or equivalently t_{DD} close to $N_{DD}T$) to single out the target ^{13}C from other environmental nuclei and then tune t_R (or *fine* tune τ) over one period $[-T_R/2, T_R/2]$ to search for large N_L . Next we perform a numerical simulation for its error tolerance.

Numerical simulation

For each set of (N_{DD}, B) , we scan t_R over one period $[-T_R/2, T_R/2]$ and scan $t_{DD} \equiv N_{DD}\tau$ (by scanning τ) in the vicinity of the resonance point $N_{DD}T$. The lifetime N_L for P1-P3 is shown in the upper panels of Fig. 5. The center of the red region correspond to diverging N_L and hence the exact QND condition. Constructing a projective measurement with readout fidelity above the threshold $\bar{\mathcal{F}}_{th} \equiv 92\%$ requires long lifetime $N_L \geq N_c$ [Eq. (19)], where N_c as a function of t_{DD} for P1-P3 is shown in the middle panel of Fig. 5. For each given t_{DD} in the (t_{DD}, t_R) plane, the width of the high-fidelity region (in which $N_L \geq N_c$) along the t_R axis, i.e., the tolerance Δt_R against systematic control error of t_R , is shown in the lower panel of Fig. 5. The worst-case estimation (dashed lines)

$$\Delta t_R \sim \frac{T_R}{\pi} \sqrt{\bar{n}C} \sin^2 \frac{\alpha}{2}$$

based on Eqs. (22)-(24) shows qualitatively similar dependences on the CPMG duration t_{DD} as the exact numerical results, but it significantly underestimate Δt_R , in agreement with our discussions in Sec. . The error tolerance Δt_R are on the nanoseconds time scale, within reach of typical experiments. Therefore, constructing projective QND measurements from a sequence of binary measurements is possible for P1-P3. Moreover, if we work at low temperatures and use resonant optical excitation for high-fidelity readout of the NV electron spin, then we can further enhance D and hence the error tolerance by a factor of ~ 18 .

CONCLUSION

We have developed a general theory for constructing projective quantum nondemolition (QND) measurement on an arbitrary nuclear spin-1/2 by measuring an auxiliary electron spin in generic electron-nuclear spin systems coupled via hyperfine interaction. A distinguishing feature is that the QND observable is *not* conserved during the free Larmor precession of the nuclear spin and can be tuned *in situ*. The key idea consists of three steps. First, suitable dynamical decoupling control on the electron is used to design the electron-nuclear entanglement and hence select the nuclear spin observable to be measured. Second, the nuclear spin evolution between neighboring measurements is tuned to make the measurement QND. Finally, a sequence of such measurements are cascaded into a projective QND measurement. We identify tunable parameters to control the QND observable and further find optimal parameters that stabilize the QND measurement against experimental control errors. This work provides a paradigm for building up QND measurement on non-conserved observables by a sequence of non-projective measurements in hybrid qubit systems, which may be relevant to the state preparation, quantum sensing, and quantum error correction via projective QND measurements. The formalisms developed here can also be used to design other QND measurements via more general quantum controls or study other measurement backaction effect in NV center and other solid-state spin systems, such as semiconductor quantum dots and phosphorus and bismuth donors in silicon.

P.W. is supported by the Talents Introduction Foundation of Beijing Normal University with Grant No.310432106. W.Y. is supported by the NSAF grant in NSFC with grant No. U1930402. P.W. and R.B.L. were supported by the Hong Kong Research Grants Council - General Research Fund Project 14300119. We acknowledge the computational support from the Beijing Computational Science Research Center (CSRC).

Note added— Recently, Ref.[52] discuss how a sequence of mutually commuting, normal POVM (which is precisely the QND condition discussed in our paper) cascade into a projective measurement and provide a simple example based on a toy model. Here we focus on a realistic physical system – electron-nuclear spin systems coupled through realistic hyperfine interaction. In this system, the electron-mediated measurement on the nuclear spin is not QND, in construct to Ref. [52]. We show how to use suitable quantum control to engineer such non-QND measurements into QND ones, how to tune the QND observables and control the strength of the QND measurements, how a sequence of such QND measurements cascade into a projective measurement, and how the QND measurement is stabilized against realistic experimental control errors. We also give an explicit scheme for constructing a projective QND measurement on a ¹³C nuclear spin weakly coupled to a nitrogen-vacancy center electron spin in diamond.

Evolution during DD sequence

We assume the DD sequence consists of N π -pulses at $t_1 \leq t_2 \leq \dots \leq t_N$. During the DD sequence, the total Hamiltonian in the interaction picture of the auxiliary electron is

$$\hat{H}(t) = [\omega + s(t)\hat{S}_z\mathbf{A}] \cdot \hat{\mathbf{I}}, \quad (26)$$

where the DD modulation function $s(t)$ starts from $s(0) = +1$ and switches its sign at t_1, t_2, \dots, t_N [40, 41]. The evolution operator during the DD sequence is $e^{-i\omega\tau}\hat{\mathbf{I}}(t_p-t_N) \dots e^{-i\omega_{\pm}\hat{\mathbf{I}}(t_3-t_2)} e^{-i\omega_{\mp}\hat{\mathbf{I}}(t_2-t_1)} e^{-i\omega_{\pm}\hat{\mathbf{I}}t_1}$

$$\hat{U}_{\text{DD}} = e^{-i(\omega+(-1)^N\hat{S}_z\mathbf{A})\hat{\mathbf{I}}} \dots e^{-i(\omega-\hat{S}_z\mathbf{A})\hat{\mathbf{I}}} e^{-i(\omega+\hat{S}_z\mathbf{A})\hat{\mathbf{I}}}. \quad (27)$$

We can expand \hat{U}_{DD} using the eigenstates $|\pm_z\rangle$ of \hat{S}_z as

$$\hat{U}_{\text{DD}} = \hat{U}_{\text{DD}}^{(+)}|+_z\rangle\langle+_z| + \hat{U}_{\text{DD}}^{(-)}|-_z\rangle\langle-_z|,$$

where $\hat{U}_{\text{DD}}^{(\pm)} = (\hat{U}_{\text{DD}})_{\hat{S}_z \rightarrow \pm 1/2}$ are nuclear spin evolution operators for the electron spin initial state $|\pm_z\rangle$. Next we define α and φ_{DD} via

$$e^{2i\alpha\hat{\mathbf{I}}} \equiv (\hat{U}_{\text{DD}}^{(+)})^\dagger \hat{U}_{\text{DD}}^{(-)},$$

$$e^{-i\varphi_{\text{DD}}\hat{\mathbf{I}}} \equiv \hat{U}_{\text{DD}}^{(+)} e^{i\alpha\hat{\mathbf{I}}} = \hat{U}_{\text{DD}}^{(-)} e^{-i\alpha\hat{\mathbf{I}}},$$

then $\hat{U}_{\text{DD}}^{(\pm)} = e^{-i\varphi_{\text{DD}}\hat{\mathbf{I}}} e^{\mp i\alpha\hat{\mathbf{I}}}$ and we obtain Eq. (2) in the main text.

Weak hyperfine interaction

The evolution operator during the DD sequence [Eq. (27)] can be written as

$$\hat{U}_{\text{DD}} = e^{-i\omega\hat{\mathbf{I}}t_{\text{DD}}}\mathcal{T}e^{-i\hat{S}_z\int_0^{t_{\text{DD}}}s(t)\mathbf{A}\cdot\hat{\mathbf{I}}(t)dt},$$

where \mathcal{T} is the time-ordering superoperator and $\hat{\mathbf{I}}(t) \equiv e^{i\omega\hat{\mathbf{I}}t}\hat{\mathbf{I}}e^{-i\omega\hat{\mathbf{I}}t}$. When the perpendicular part \mathbf{A}_\perp of \mathbf{A} with respect to ω is much smaller than the nuclear Zeeman splitting $|\omega|$, we can use the first-order Magnus expansion to obtain

$$\hat{U}_{\text{DD}} \approx e^{-i\omega\hat{\mathbf{I}}t_{\text{DD}}} e^{-i\hat{S}_z\int_0^{t_{\text{DD}}}s(t)\mathbf{A}\cdot\hat{\mathbf{I}}(t)dt}.$$

For convenience we define ω as the z axis ($\omega = \omega\mathbf{e}_z$) and decompose \mathbf{A} into $A_z\mathbf{e}_z$ and $\mathbf{A}_\perp = A_\perp(\cos\Phi\mathbf{e}_x + \sin\Phi\mathbf{e}_y) = A_\perp\text{Re}\mathbf{e}_+e^{-i\Phi}$ ($\mathbf{e}_\pm \equiv \mathbf{e}_x \pm i\mathbf{e}_y$), then $\mathbf{A} \cdot \hat{\mathbf{I}}(t) = A_z\hat{I}_z + A_\perp\hat{\mathbf{I}} \cdot \text{Re}\mathbf{e}_+e^{-i\Phi}e^{i\omega t}$. For a DD sequence of duration t_{DD} , the modulation function must satisfy $\int_0^{t_{\text{DD}}}s(t)dt = 0$, thus the term $A_z\hat{I}_z$ is averaged out, and

$$\hat{U}_{\text{DD}} \approx e^{-\omega t_{\text{DD}}\hat{I}_z} e^{-i\hat{S}_z t_{\text{DD}} A_\perp \hat{\mathbf{I}} \cdot \text{Re}\mathbf{e}_+ e^{-i\Phi} f_{\text{DD}}} = e^{-it_{\text{DD}}(\omega\hat{\mathbf{I}})} e^{-i2\hat{S}_z\alpha\hat{\mathbf{I}}},$$

where f_{DD} is given by Eq. (12) and α is given by Eq. (11).

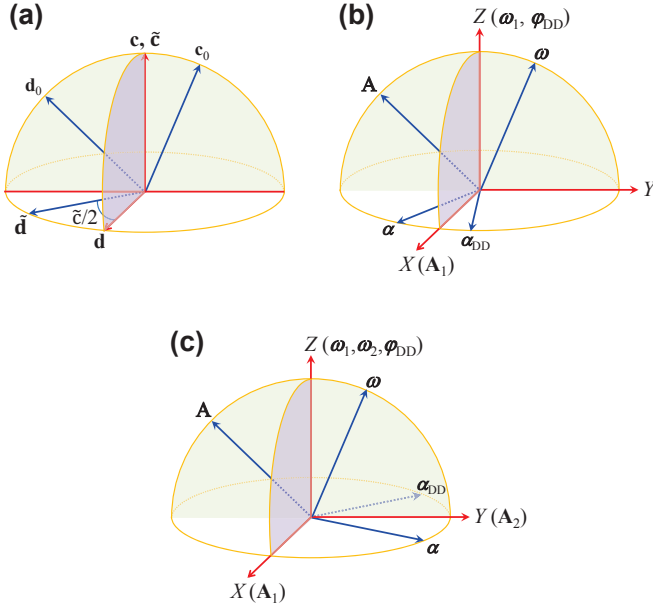


FIG. 6. (a) Orientation of relevant vectors for Eqs. (29) and (30). (b) Orientations of relevant vectors for the periodic DD. (c) Orientations of relevant vectors for the CPMG sequence.

Stroboscopic QND condition for even-order concatenated DD sequences

The QND condition Eq. (14) is equivalent to

$$\mathbb{R}(\varphi_R)\hat{\alpha}_{\text{DD}} = \hat{\alpha}, \quad (28)$$

where $\hat{\alpha}_{\text{DD}} \equiv \mathbb{R}(\varphi_{\text{DD}})\hat{\alpha}$ is obtained from $\hat{\alpha}$ by a rotation around the axis φ_{DD} by an angle $|\varphi_{\text{DD}}|$. This can be achieved by first tuning the direction of φ_R into the *bisection plane* of $\hat{\alpha}$ and $\hat{\alpha}_{\text{DD}}$ and then tuning $|\varphi_R|$ to satisfy Eq. (28). As discussed in the main text, we can achieve an *arbitrary* evolution $e^{-i\varphi_R\hat{\mathbf{I}}}$ by tuning t_R and the timings of the electron spin flip during the waiting time t_R , so Eq. (28) can always be satisfied. Next, we further prove that when the DD sequence is the repetition of an *even-order* concatenated DD [43–46], the QND condition can be achieved by the evolution $e^{-i\varphi_R\hat{\mathbf{I}}} = e^{-i(\omega+\mathbf{A}/2)t_R\hat{\mathbf{I}}}$ at suitable t_R , i.e., for these DD sequences, the QND condition can be satisfied by tuning the duration t_R of the waiting interval, without flipping the electron spin during the waiting interval.

We will use repeatedly two important properties (with \hat{S}_z for the electron spin-1/2 and $\hat{\mathbf{I}}$ for the target nuclear spin-1/2): (i) Given arbitrary vectors \mathbf{c}_0 and \mathbf{d}_0 , if we define \mathbf{c} and \mathbf{d} via

$$e^{-i(\mathbf{c}+\hat{S}_z\mathbf{d})\hat{\mathbf{I}}} = e^{-i(\mathbf{c}_0-\hat{S}_z\mathbf{d}_0)\hat{\mathbf{I}}}e^{-i(\mathbf{c}_0+\hat{S}_z\mathbf{d}_0)\hat{\mathbf{I}}}, \quad (29)$$

then \mathbf{c} lies in the \mathbf{c}_0 - \mathbf{d}_0 plane ($\mathbf{c} \parallel \mathbf{c}_0$ if $\mathbf{c}_0 \perp \mathbf{d}_0$), while $\mathbf{d} \parallel \mathbf{c}_0 \times \mathbf{d}_0$, as shown in Fig. 6(a). (ii) Given two orthogonal vectors $\mathbf{c} \perp \mathbf{d}$, if we define $\tilde{\mathbf{c}}$ and $\tilde{\mathbf{d}}$ via

$$e^{-i\tilde{\mathbf{c}}\hat{\mathbf{I}}}e^{-i2\hat{S}_z\tilde{\mathbf{d}}\hat{\mathbf{I}}} = e^{-i(\mathbf{c}+\hat{S}_z\mathbf{d})\hat{\mathbf{I}}}, \quad (30)$$

then $\tilde{\mathbf{c}} \parallel \mathbf{c}$ and $\tilde{\mathbf{d}} \parallel \mathbb{R}(-\tilde{\mathbf{c}}/2)\mathbf{d}$, as shown in Fig. 6(a). The proof will be given at the end of this appendix.

To illustrate the concept of concatenation, we begin with the periodic DD $(\tau/4-\pi-\tau/4-\pi)^N$ consisting of N periods. The evolution operator \hat{U}_1 of the electron-nuclear system in one period is the concatenation of the free evolution $\hat{U}_0 \equiv e^{-i(\tau/4)(\omega+\hat{S}_z\mathbf{A})\hat{\mathbf{I}}}$, i.e.,

$$\hat{U}_1 \equiv (\hat{U}_0)_{\hat{S}_z \rightarrow -\hat{S}_z} \hat{U}_0, \quad (31)$$

and the total evolution during this DD sequence is $\hat{U}_{\text{DD}} = \hat{U}_1^N$. Namely, this periodic DD consists of N repetitions of the *first-order* concatenated DD. Using Eq. (29), we have

$$\begin{aligned} \hat{U}_1 &= e^{-i(\tau/2)(\omega_1+\hat{S}_z\mathbf{A}_1/2)\hat{\mathbf{I}}}, \\ \hat{U}_{\text{DD}} &= e^{-i(N\tau/2)(\omega_1+\hat{S}_z\mathbf{A}_1/2)\hat{\mathbf{I}}}, \end{aligned}$$

where ω_1 lies in the ω - \mathbf{A} plane and $\mathbf{A}_1 \parallel \omega \times \mathbf{A}$. For convenience, we define \mathbf{A}_1 as the X axis, the ω - \mathbf{A} plane as the YZ plane, and ω_1 as the Z axis, as shown in Fig. 6(b). Next we can use Eq. (30) to obtain $\hat{U}_{\text{DD}} = e^{-i\varphi_{\text{DD}}\hat{\mathbf{I}}}e^{-i2\hat{S}_z\alpha\hat{\mathbf{I}}}$ with φ_{DD} along the Z axis and $\hat{\alpha}$ in the XY plane with azimuth $-|\varphi_{\text{DD}}|/2$, so $\hat{\alpha}_{\text{DD}}$ also lies in the XY plane with azimuth $|\varphi_{\text{DD}}|/2$, i.e., $\hat{\alpha}$ and $\hat{\alpha}_{\text{DD}}$ lie symmetrically about \mathbf{A}_1 in the XY plane, as shown in Fig. 6(b). Therefore, for the periodic DD, the evolution $e^{-i\varphi_R\hat{\mathbf{I}}} = e^{-i(\omega+\mathbf{A}/2)t_R\hat{\mathbf{I}}}$ cannot satisfy the QND condition.

Next we consider the CPMG sequence $(\tau/4-\pi-\tau/2-\pi-\tau/4)^N$ consisting of N periods. The evolution operator of the electron-nuclear system during one period is the concatenation of \hat{U}_1 [Eq. (31)], i.e.,

$$\hat{U}_2 \equiv (\hat{U}_1)_{\hat{S}_z \rightarrow -\hat{S}_z} \hat{U}_1,$$

and the total evolution during the CPMG sequence is $\hat{U}_{\text{DD}} = \hat{U}_2^N$. Namely, this CPMG sequence consists of N repetitions of the *second-order* concatenated DD. Using Eq. (29), we obtain

$$\hat{U}_2 = e^{-i\tau(\omega_2+\hat{S}_z\mathbf{A}_2/2)\hat{\mathbf{I}}},$$

with ω_2 along the Z axis and \mathbf{A}_2 along the Y axis. Next we use Eq. (30) to obtain $\hat{U}_{\text{DD}} = e^{-i\varphi_{\text{DD}}\hat{\mathbf{I}}}e^{-i2\hat{S}_z\alpha\hat{\mathbf{I}}}$ with φ_{DD} along the Z axis and $\hat{\alpha}$ in the XY plane with azimuth $\pi/2-|\varphi_{\text{DD}}|/2$, so $\hat{\alpha}_{\text{DD}}$ also lies in the XY plane with azimuth $\pi/2+|\varphi_{\text{DD}}|/2$, i.e., $\hat{\alpha}$ and $\hat{\alpha}_{\text{DD}}$ lie symmetrically about \mathbf{A}_2 in the XY plane [see Fig. 6(c)]. Then the evolution $e^{-i\varphi_R\hat{\mathbf{I}}} = e^{-i(\omega+\mathbf{A}/2)t_R\hat{\mathbf{I}}}$ can satisfy the stroboscopic QND condition at suitable t_R , i.e., without flipping the electron spin during the waiting time.

The concatenation process can be carried out to higher order to obtain the period

$$\hat{U}_l \equiv (\hat{U}_{l-1})_{\hat{S}_z \rightarrow -\hat{S}_z} \hat{U}_{l-1}$$

of the l th-order concatenated DD [43–46]. If the DD sequence consists of N repetitions of \hat{U}_l , then the total evolution is $\hat{U}_{\text{DD}} = \hat{U}_l^N$. Using Eq. (29), we obtain

$$\hat{U}_l = e^{-i2^{l-2}N\tau(\omega_l+\hat{S}_z\mathbf{A}_l)\hat{\mathbf{I}}},$$

with ω_l along the Z axis and \mathbf{A}_l in the XY plane with azimuth $(l-1)\pi/2$. Next we can use Eq. (30) to obtain

$\hat{U}_{\text{DD}} = e^{-i\varphi_{\text{DD}}\hat{\mathbf{I}}}e^{-i2\delta_s\alpha\hat{\mathbf{I}}}$, where φ_{DD} is along the Z axis and $\hat{\alpha}$ in the XY plane with azimuth $(l-1)\pi/2 - |\varphi_{\text{DD}}|/2$, so $\hat{\alpha}_{\text{DD}}$ also lies in the XY plane with azimuth $(l-1)\pi/2 + |\varphi_{\text{DD}}|/2$, i.e., $\hat{\alpha}$ and $\hat{\alpha}_{\text{DD}}$ lie symmetrically about \mathbf{A}_l in the XY plane. For even l , \mathbf{A}_l is along the $\pm Y$ axis, so the evolution $e^{-i\varphi_R\hat{\mathbf{I}}} = e^{-i(\omega+\mathbf{A}/2)\hat{\mathbf{I}}t_R}$ can satisfy the stroboscopic QND condition at suitable t_R , i.e., without flipping the electron spin during the waiting time.

Finally we prove properties (i) and (ii). For property (i), we notice that Eq. (29) is equivalent to

$$e^{-i(\mathbf{c}\pm\mathbf{d}/2)\hat{\mathbf{I}}} = e^{-i(\mathbf{c}_0\mp\mathbf{d}_0/2)\hat{\mathbf{I}}}e^{-i(\mathbf{c}_0\pm\mathbf{d}_0/2)\hat{\mathbf{I}}},$$

which further becomes

$$e^{-i(\mathbf{C}\pm\mathbf{D})\cdot\boldsymbol{\sigma}} = e^{-i\mathbf{a}_+\cdot\boldsymbol{\sigma}}e^{-i\mathbf{a}_-\cdot\boldsymbol{\sigma}}$$

by using $\hat{\mathbf{I}} = \boldsymbol{\sigma}/2$ ($\boldsymbol{\sigma}$ are Pauli matrices) and defining $\mathbf{C} \equiv \mathbf{c}/2$, $\mathbf{D} = \mathbf{d}/4$, and $\mathbf{a}_{\pm} \equiv (\mathbf{c}_0 \pm \mathbf{d}_0/2)/2$. Using $e^{-i\theta(\mathbf{e}\cdot\boldsymbol{\sigma})} = \cos\theta - i\boldsymbol{\sigma}\cdot\sin(\theta\mathbf{e})$ [\mathbf{e} is a unit vector and $\sin(\theta\mathbf{e}) \equiv \mathbf{e}\sin\theta$], we obtain

$$\begin{aligned}\cos|\mathbf{C}\pm\mathbf{D}| &= \cos a_+ \cos a_- - \sin a_+ \cdot \sin a_-, \\ \sin(\mathbf{C}\pm\mathbf{D}) &= \cos a_+ \sin a_- + \sin a_+ \cos a_- \pm \sin a_- \times \sin a_+, \end{aligned}$$

where $a_{\pm} = |\mathbf{a}_{\pm}|$. The first equation dictates $|\mathbf{C} + \mathbf{D}| = |\mathbf{C} - \mathbf{D}|$, then we can substitute $\sin(\mathbf{C}\pm\mathbf{D}) = (\mathbf{C}\pm\mathbf{D}) \text{sinc} \sqrt{C^2 + D^2}$ into the second equation to obtain $\mathbf{C} \propto \sin a_- \cos a_+ + \sin a_+ \cos a_-$ and $\mathbf{D} \propto \sin a_- \times \sin a_+$. In other words, \mathbf{C} lies in the \mathbf{a}_+ - \mathbf{a}_- plane ($\mathbf{C} \parallel \mathbf{a}_+ + \mathbf{a}_-$ if $a_+ = a_-$), while $\mathbf{D} \parallel \mathbf{a}_- \times \mathbf{a}_+$. This proves property (i).

Similarly, Eq. (30) is equivalent to

$$e^{-i\tilde{\mathbf{c}}\hat{\mathbf{I}}}e^{\mp i\tilde{\mathbf{d}}\hat{\mathbf{I}}} = e^{-i(\tilde{\mathbf{c}}\pm\tilde{\mathbf{d}}/2)\hat{\mathbf{I}}},$$

which further becomes

$$e^{-i\tilde{\mathbf{C}}\cdot\boldsymbol{\sigma}}e^{\mp i\tilde{\mathbf{D}}\cdot\boldsymbol{\sigma}} = e^{-i(\mathbf{C}\pm\mathbf{D})\cdot\boldsymbol{\sigma}}$$

with $\mathbf{C} = \tilde{\mathbf{c}}/2$, $\mathbf{D} = \tilde{\mathbf{d}}/4$, $\tilde{\mathbf{C}} = \tilde{\mathbf{c}}/2$, and $\tilde{\mathbf{D}} = \tilde{\mathbf{d}}/2$. Using $e^{-i\theta(\mathbf{e}\cdot\boldsymbol{\sigma})} = \cos\theta - i\boldsymbol{\sigma}\cdot\sin(\theta\mathbf{e})$, we obtain

$$\cos \sqrt{C^2 + D^2} = \cos \tilde{C} \cos \tilde{D} \mp \sin \tilde{C} \cdot \sin \tilde{D},$$

$$(\mathbf{C}\pm\mathbf{D}) \text{sinc} \sqrt{C^2 + D^2} = \sin \tilde{C} \cos \tilde{D} \pm \sin \tilde{D} \cos \tilde{C} \pm \sin \tilde{C} \times \sin \tilde{D}.$$

The first equation dictates $\tilde{\mathbf{C}} \perp \tilde{\mathbf{D}}$. The second equation gives $\mathbf{C} \propto \sin \tilde{C}$ and $\mathbf{D} \propto \sin \tilde{D} \cos \tilde{C} + \sin \tilde{C} \times \sin \tilde{D} = \mathbb{R}(\tilde{\mathbf{C}}) \sin \tilde{D}$, so $\tilde{\mathbf{C}} \parallel \mathbf{C}$ and $\tilde{\mathbf{D}} \parallel \mathbb{R}(-\tilde{\mathbf{C}})\mathbf{D}$. This proves property (ii).

* wenyang@csrc.ac.cn

† rbliu@cuhk.edu.hk

- [1] H. M. Wiseman and G. J. Milburn, *Quantum measurement and control* (Cambridge University Press, 2010).
 [2] V. B. Braginsky and Y. I. Vorontsov, *Soviet Physics Uspekhi* **17**, 644 (1975).
 [3] V. Braginskii, Y. I. Vorontsov, and F. Y. Khalili, *Sov. Phys. JETP* **46**, 705 (1977).

- [4] K. S. Thorne, R. W. P. Drever, C. M. Caves, M. Zimmermann, and V. D. Sandberg, *Phys. Rev. Lett.* **40**, 667 (1978).
 [5] W. G. Unruh, *Phys. Rev. D* **19**, 2888 (1979).
 [6] C. M. Caves, K. S. Thorne, R. W. P. Drever, V. D. Sandberg, and M. Zimmermann, *Rev. Mod. Phys.* **52**, 341 (1980).
 [7] V. B. Braginsky, Y. I. Vorontsov, and K. S. Thorne, *Science* **209**, 547 (1980).
 [8] A. A. Clerk, M. H. Devoret, S. M. Girvin, F. Marquardt, and R. J. Schoelkopf, *Rev. Mod. Phys.* **82**, 1155 (2010).
 [9] P. Grangier, J. A. Levenson, and J.-P. Poizat, *Nature* **396**, 537 (1998).
 [10] A. Lupascu, S. Saito, T. Picot, P. C. de Groot, C. J. P. M. Harmans, and J. E. Mooij, *Nat. Phys.* **3**, 119 (2007).
 [11] S. Peil and G. Gabrielse, *Phys. Rev. Lett.* **83**, 1287 (1999).
 [12] A. Laraoui, F. Dolde, C. Burk, F. Reinhard, J. Wrachtrup, and C. A. Meriles, *Nature Communications* **4**, 1651 (2013).
 [13] T. Staudacher, N. Raatz, S. Pezzagna, J. Meijer, F. Reinhard, C. A. Meriles, and J. Wrachtrup, *Nat. Commun.* **6**, (2015).
 [14] H. J. Mamin, M. Kim, M. H. Sherwood, C. T. Rettner, K. Ohno, D. D. Awschalom, and D. Rugar, *Science* **339**, 557 (2013).
 [15] Z.-Y. Wang, J. Casanova, and M. B. Plenio, *Nat. Commun.* **8**, 14660 (2017).
 [16] S. Zaiser, T. Rendler, I. Jakobi, T. Wolf, S.-Y. Lee, S. Wagner, V. Bergholm, T. Schulte-Herbrüggen, P. Neumann, and J. Wrachtrup, *Nature Communications* **7**, 12279 (2016).
 [17] F. Shi, X. Kong, P. Wang, F. Kong, N. Zhao, R.-B. Liu, and J. Du, *Nat. Phys.* **10**, 21 (2014).
 [18] F. Shi, Q. Zhang, P. Wang, H. Sun, J. Wang, X. Rong, M. Chen, C. Ju, R. Friedemann, J. Wang, and J. Du, *Science* **347**, 1135 (2015).
 [19] J. Du, X. Rong, N. Zhao, Y. Wang, J. Yang, and R. B. Liu, *Nature* **461**, 1265 (2009).
 [20] M. Pfender, N. Aslam, H. Sumiya, S. Onoda, P. Neumann, J. Isoya, C. A. Meriles, and J. Wrachtrup, *Nat. Commun.* **8**, 834 (2017).
 [21] T. Rosskopf, J. Zopes, J. M. Boss, and C. L. Degen, *npj Quantum Inf.* **3**, 33 (2017).
 [22] S. Schmitt, T. Gefen, F. M. Stürner, T. Uden, G. Wolff, C. Müller, J. Scheuer, B. Naydenov, M. Markham, S. Pezzagna, J. Meijer, I. Schwarz, M. Plenio, A. Retzker, L. P. McGuinness, and F. Jelezko, *Science* **356**, 832 (2017).
 [23] D. R. Glenn, D. B. Bucher, J. Lee, M. D. Lukin, H. Park, and R. L. Walsworth, *Nature* **555**, 351 (2018).
 [24] J. T. Muhonen, J. P. Dehollain, A. Laucht, F. E. Hudson, R. Kalra, T. Sekiguchi, K. M. Itoh, D. N. Jamieson, J. C. McCallum, A. S. Dzurak, and A. Morello, *Nat Nano* **9**, 986 (2014).
 [25] K. Saeedi, S. Simmons, J. Z. Salvail, P. Dluhy, H. Riemann, N. V. Abrosimov, P. Becker, H.-J. Pohl, J. J. Morton, and M. L. Thewalt, *Science* **342**, 830 (2013).
 [26] A. M. Tyryshkin, S. Tojo, J. J. L. Morton, H. Riemann, N. V. Abrosimov, P. Becker, H.-J. Pohl, T. Schenkel, M. L. W. Thewalt, K. M. Itoh, and S. A. Lyon, *Nat. Mater.* **11**, 143 (2012).
 [27] D. Press, K. De Greve, P. L. McMahon, T. D. Ladd, B. Friess, C. Schneider, M. Kamp, S. Hofling, A. Forchel, and Y. Yamamoto, *Nat. Photon.* **4**, 367 (2010).
 [28] T. H. Taminiau, J. Cramer, T. van der Sar, V. V. Dobrovitski, and R. Hanson, *Nat Nano* **9**, 171 (2014).
 [29] S. Yang, Y. Wang, D. D. B. Rao, T. Hien Tran, A. S. Momenzadeh, M. Markham, D. J. Twitchen, P. Wang, W. Yang, R. Stöhr, P. Neumann, H. Kosaka, and J. Wrachtrup, *Nature Photonics* **10**, 507 (2016).
 [30] A. Dreau, P. Spinicelli, J. R. Maze, J.-F. Roch, and V. Jacques, *Phys. Rev. Lett.* **110**, 060502 (2013).
 [31] P. Neumann, J. Beck, M. Steiner, F. Rempp, H. Fedder, P. R.

- Hemmer, J. Wrachtrup, and F. Jelezko, *Science* **329**, 542 (2010).
- [32] G.-Q. Liu, J. Xing, W.-L. Ma, P. Wang, C.-H. Li, H. C. Po, Y.-R. Zhang, H. Fan, R.-B. Liu, and X.-Y. Pan, *Phys. Rev. Lett.* **118**, 150504 (2017).
- [33] V. B. Braginsky, Y. I. Vorontsov, and F. Y. Khalili, *JETP Lett.* **27**, 276 (1978).
- [34] A. N. Jordan and M. Büttiker, *Phys. Rev. B* **71**, 125333 (2005).
- [35] R. Ruskov, K. Schwab, and A. N. Korotkov, *Phys. Rev. B* **71**, 235407 (2005).
- [36] A. N. Jordan, A. N. Korotkov, and M. Büttiker, *Phys. Rev. Lett.* **97**, 026805 (2006).
- [37] D. V. Averin, K. Rabenstein, and V. K. Semenov, *Phys. Rev. B* **73**, 094504 (2006).
- [38] A. N. Jordan and A. N. Korotkov, *Phys. Rev. B* **74**, 085307 (2006).
- [39] J. N. Greiner, D. B. R. Dasari, and J. Wrachtrup, *Sci. Rep.* **7**, 529 (2017).
- [40] L. Cywinski, R. M. Lutchyn, C. P. Nave, and S. Das Sarma, *Phys. Rev. B* **77**, 174509 (2008).
- [41] W. Yang, W.-L. Ma, and R.-B. Liu, *Rep. Prog. Phys.* **80**, 016001 (2017).
- [42] R.-B. Liu, W. Yao, and L. J. Sham, *Adv. Phys.* **59**, 703 (2010).
- [43] K. Khodjasteh and D. A. Lidar, *Phys. Rev. Lett.* **95**, 180501 (2005).
- [44] W. Yao, R.-B. Liu, and L. J. Sham, *Phys. Rev. Lett.* **98**, 077602 (2007).
- [45] K. Khodjasteh and D. A. Lidar, *Phys. Rev. A* **75**, 062310 (2007).
- [46] W. Yang, Z.-Y. Wang, and R.-B. Liu, *Front. Phys.* **6**, 2 (2011).
- [47] L. Robledo, L. Childress, H. Bernien, B. Hensen, P. F. A. Alkemade, and R. Hanson, *Nature* **477**, 574 (2011).
- [48] W. Pfaff, T. H. Taminiau, L. Robledo, H. Bernien, M. Markham, D. J. Twitchen, and R. Hanson, *Nat. Phys.* **9**, 29 (2013).
- [49] J. Cramer, N. Kalb, M. A. Rol, B. Hensen, M. S. Blok, M. Markham, D. J. Twitchen, R. Hanson, and T. H. Taminiau, *Nat. Commun.* **7**, 11526 (2016).
- [50] N. Kalb, J. Cramer, D. J. Twitchen, M. Markham, R. Hanson, and T. H. Taminiau, *Nat. Commun.* **7**, 13111 (2016).
- [51] A. Reiserer, N. Kalb, M. S. Blok, K. J. M. van Bemmelen, T. H. Taminiau, R. Hanson, D. J. Twitchen, and M. Markham, *Phys. Rev. X* **6**, 021040 (2016).
- [52] W.-L. Ma, S.-S. Li, and R.-B. Liu, *arXiv:2208.08141v1* (2022).